

AN ELECTRON BOMBARDMENT FURNACE
AN ELECTRODYNAMOMETER FOR THE
MEASUREMENT OF SMALL FORCES

by

JAMES PHILLIP DAWSON

"


Bachelor of Science
Southwestern State College
Weatherford, Oklahoma
1955

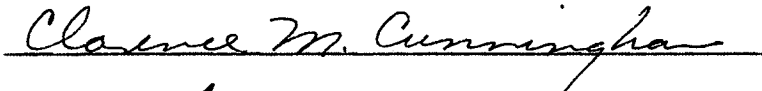
Submitted to the faculty of the Graduate School of
the Oklahoma State University in partial
fulfillment of the requirements
for the degree of
MASTER OF SCIENCE
May, 1960

SEP 1 1930

AN ELECTRON BOMBARDMENT FURNACE
AN ELECTRODYNAMOMETER FOR THE
MEASUREMENT OF SMALL FORCES

Thesis Approved:


Thesis Adviser




Dean of the Graduate School

452697

ACKNOWLEDGMENT

The author wishes to express his sincerest appreciation to Dr. Robert D. Freeman for his encouragement and guidance throughout these studies. Also the author is grateful to Mr. Heinz Hall for his excellent craftsmanship in constructing the Electrodynamometer, and to Professor Paul A. McCollum for his guidance in designing the Electron Bombardment Furnace.

The author is also grateful to the United States Air Force Office of Scientific Research and to the Oklahoma State University Research Foundation for financial support of this research.

TABLE OF CONTENTS

Part	Page
I. THE ELECTRON BOMBARDMENT FURNACE.	1
Introduction	1
Control Circuit.	3
Power Supply	3
Apparatus.	7
Performance.	7
II. THE TORSION TEST SYSTEM	10
Introduction	10
Apparatus.	12
Control Circuit.	16
Experimental	18
III. THE ELECTRODYNAMOMETER.	23
Introduction	23
Stationary Coil.	24
Movable Coil	32
Suspension Adjustments	33
Suspension Wire.	36
Cubical Mirror	39
Control Circuit.	41
Experimental	45
SELECTED BIBLIOGRAPHY	

LIST OF TABLES

Table	Page
I. Components of the Power Supply for the Electron Bombardment Furnace	8
II. Data Obtained with Torsion Test System.	20
III. Diameters of the Stationary Coil.	25
IV. Breadth of the "d" Sections of the Stationary Coil.	27
V. Average Breadth of the "d" Sections of the Stationary Coil.	28
VI. The Breadth and the Location of Each Section of Winding and Its Magnetic Force at the Center of the Stationary Coil	29
VII. Wire Displacements for Openings in the Stationary Coil.	31
VIII. Diameters of the Movable Coil	33
IX. Length of Winding of the Movable Coil	33
X. Dimensions of Brass Cylinder.	37
XI. Periods of Oscillation for Suspension Wire.	38
XII. Calibration Data for Cubical Mirror	40
XIII. Values of the Angles on Cubical Mirror.	41
XIV. Comparison of Current Measured by Electrodynamometer and by the Potentiometer-Resistor Method	46

LIST OF FIGURES

Figure	Page
1. Control Circuit for Electron Bombardment Furnace	4
2. Power Supply for Electron Bombardment Furnace.	5
3. Modified Leeds and Northrup Galvanometer	13
4. Vacuum Chamber for Torsion Test System	14
5. Effusion Cell and Collimator of Torsion Test System.	15
6. Control Circuit for Torsion Test System.	17
7. Torsion Test System Calibration Data	21
8. Breadth of "d" Sections on Stationary Coil	25
9. Winding Displacements on Stationary Coil	31
10. Suspension Adjustments	34
11. Degrees of Freedom of Stationary Coil.	36
12. Brass Cylinder for Calibration of Suspension Wires	38
13. Telescope Arrangement for Calibration of Cubical Mirror.	40
14. Electrical Connections to Movable Coil	42
15. Control Circuit for the Electrodynamometer	44

PART I

THE ELECTRON BOMBARDMENT FURNACE

Introduction

Electron bombardment furnaces have been operated successfully for extended periods in high temperature, high vacuum studies. Electron bombardment heating has advantages over induction heating for two reasons: the power supply is relative simple and inexpensive and the temperature may be easily controlled over a wide range. Resistance heating has the definite disadvantage of complexity of furnace design for extreme temperatures.

Generally, electron bombardment is considered to be the removal of electrons from a metal and the direction of them to the surface of the object to be heated. When an electron is removed from a metal, work must be done against the attractive forces which normally prevent its escape. The work per unit charge required to remove an electron from a metal is called the work function of the metallic surface and is of the order of magnitude of a few volts. This work must be done no matter what method of liberation is employed, various methods differing in the manner in which the requisite energy is supplied to the escaping electron. In the photoelectric effect, the electrons gain energy from the absorption of light. Electrons liberated by bombarding a metal with secondary electrons pick up their excess energy from the impinging electrons. Bombardment by positive ions or by neutral atoms carrying more than their normal configuration

energies (meta-stable atoms) can also liberate electrons. Very intense electric fields can pull electrons out of metals (cold emission) and finally, heating the metal can impart sufficient thermal energy to some of the electrons to enable their escape in a manner analogous to the thermal evaporation of a liquid. The latter method is the one employed in this furnace. This phenomenon of thermionic emission or electron bombardment heating has become commonplace through application to the outgassing stage in the manufacture of vacuum tubes. This method of obtaining high temperatures has also been used for laboratory purposes and is currently under commercial development for use in purification of metals such as titanium, niobium, tantalum, etc.

The problem of temperature control is usually the limiting factor in any furnace design. In the electron bombardment furnace the current is controlled by the temperature and work function of the emitter filament. While the filament temperature is directly controlled by the filament current, the work function is subject to uncontrolled variation. The work function is dependent of the nature and degree of absorption of gases in the vacuum system. If the temperature decreases, the rate of gas evolution decreases and the work function diminishes. The emission current increases and the temperature rises. This temperature oscillation is frequently undamped and divergent, making manual control of the furnace tedious and time consuming.

Rocco and Sears (16) have described an electron bombardment furnace controller which has been successfully operated over a range of temperatures from room temperature to 2100°K. The constancy of temperature over a several hour period was approximately 0.1% at 1600-1800°C. The power supply for their furnace was a commercial unit designed to

supply 0-500 ma. at constant voltage over the range of 200-1000 volts. The crucible used by Rocco and Sears was 0.625 inch O.D.; 0.375 inch I.D. and 0.575 inch in length. Their electron emission filament consisted of a 5-turn helix of 0.020-inch diameter tungsten wire wound to a 0.25-inch O.D.

Control Circuit

The temperature control circuit is shown diagrammatically in Figure 1. The control problem was simplified by the condition that the current could undergo short-term fluctuations. Only the time average current was maintained constant.

The control signal was obtained by passing the bombardment current through a precision resistor. The voltage signal across this resistor was fed into a servo-amplifier, whose cross-over voltage was controlled by a ten-turn potentiometer, R-12, fed by a constant voltage supply. The output of the servo-amplifier controlled a servo-motor such that the filament current was reduced when the bombardment current increased above the control value and vice versa. Only a fraction of the filament heating current was supplied through the servo-controlled Variac, W-2. The major portion of the filament current was supplied through a manually operated Variac, V-20.

Power Supply

The circuit for the power supply of the electron bombardment furnace is shown diagrammatically in Figure 2. The initial input to the circuit is through a Stabiline voltage regulator type EM 4106, which supplies 115 volts and is rated at 6.0 KVA. The output of the power supply is 0-3000 VDC and 0-1000 ma in any combination.

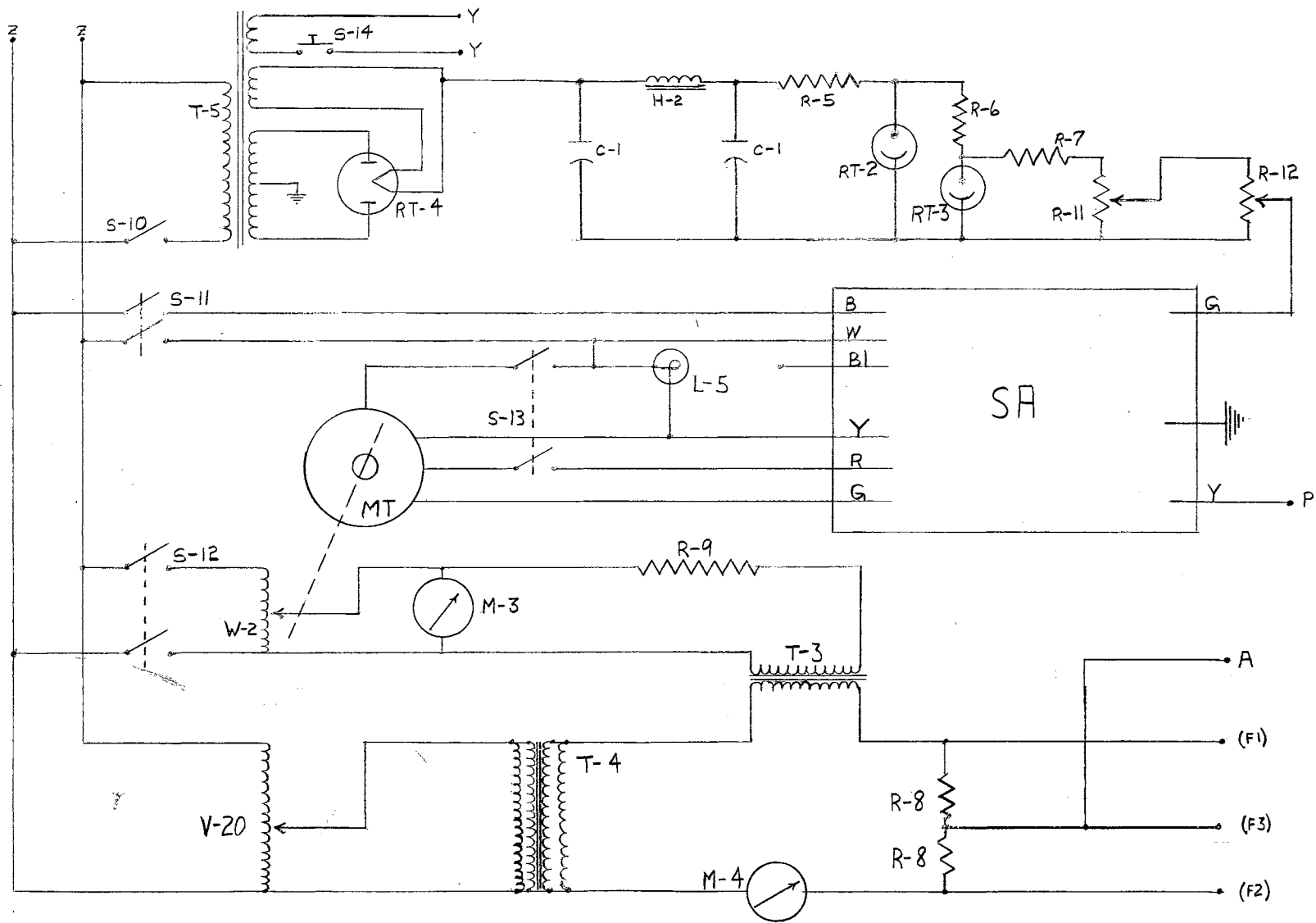


Figure 1. Control Circuit for the Electron Bombardment Furnace

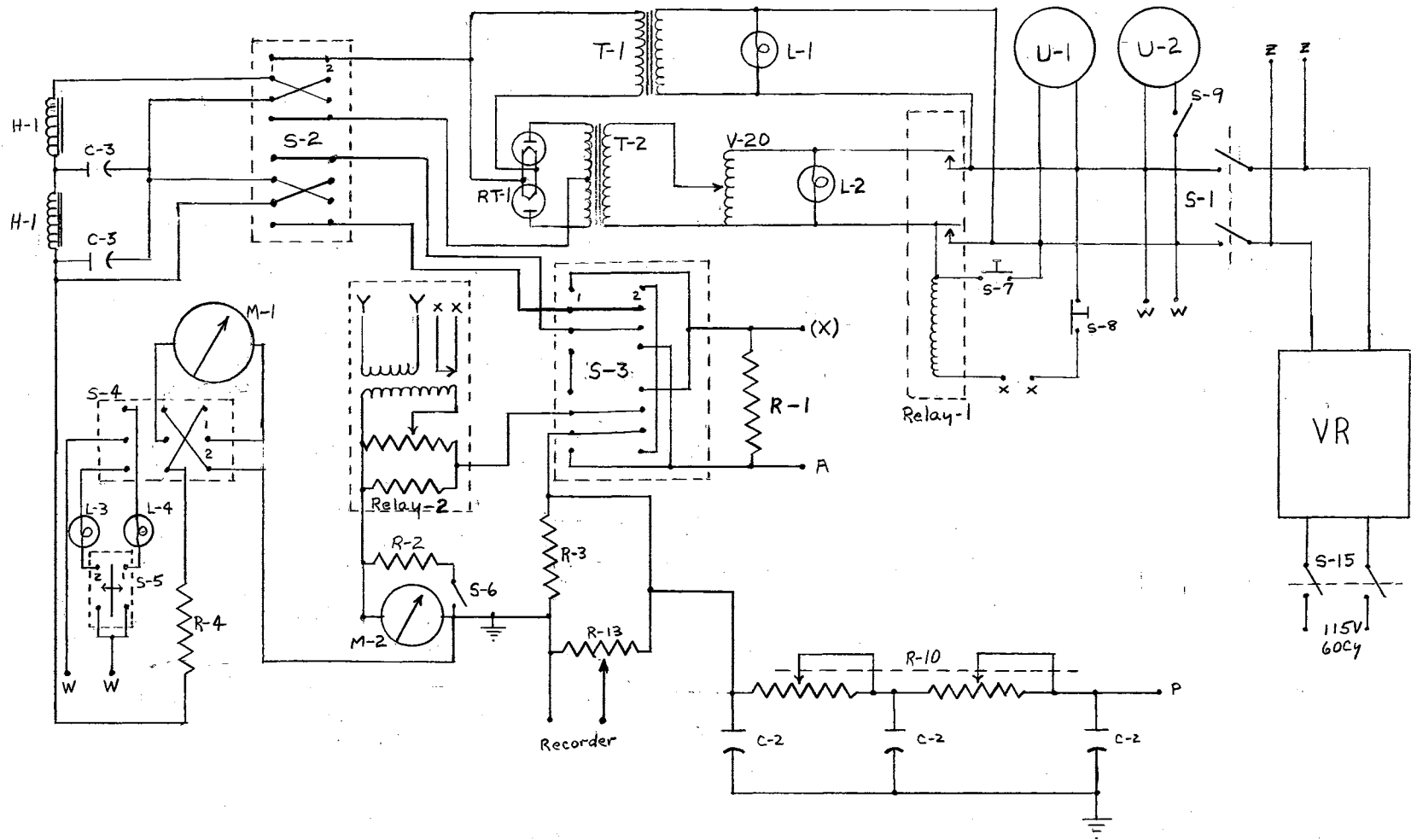


Figure 2. Power Supply for the Electron Bombardment Furnace

Switch S-1 is the main circuit breaker. When S-1 is thrown the light L-1 comes on indicating that the rectifier tubes are warming up. Also, the time totalizer is turned on. Another timer, which counts seconds and is equipped with reset, enables the operator to time individual runs. The second timer is operated by switch S-9.

Switch S-7 (high voltage ON button, black) energizes the power relay (relay-1) turning on the high voltage, indicated by L-2. Voltage to the transformer T-2 is controlled by Variac W-20. Switches S-2 and S-3 are high voltage switches constructed in this laboratory. The position of S-3 determines whether the crucible or the filament is grounded and S-2 permits the chokes, H-1, to be kept on the ungrounded side. Switch S-4 adjusts the polarity of the connections to the 0-3000 volt-meter to compensate for operation of S-2 and S-3. Switch S-5 is operated by a cam connected to the shaft of switch S-3. When the switches S-2, S-3, S-4 and S-5 are all in the same position, the indicator light (L-3, position 2; L-4, position 1) comes on. When the switch on the voltage regulator, S-15, is thrown and the polarity switches are all in either position one or position two, the corresponding indicator light is on. This allows the operator to have the correct setting on the polarity switches even before any of the power supply circuits are energized through switch S-1.

The 0-500 milliammeter has the resistance R-2 in parallel. The value of R-2 is equal to the internal resistance of the milliammeter and effectively doubles the range of the meter. Switch S-6 operates the parallel circuit allowing full scale deflection of the meter at 500 and 1000 ma. The relay-2 is a protective overload relay adjusted to de-energize the high voltage circuit if the emission current exceeds

1100 ma. The overload reset is operated by switch S-41 connected at "y-y" as shown in the diagram.

Apparatus

The vacuum system used in conjunction with the electron bombardment furnace has been described by W. F. Heydman (8). The design and operation of the filament, radiation shields, etc., will be discussed by J. E. Bennett in his Masters Thesis.

Performance

The furnace temperature was measured with a Leeds and Northrup Type 8622-C optical pyrometer. The furnace was controlled at 1608°K for a period of one hour with no apparent fluctuations in temperature. The highest temperature attained with the furnace was 2173°K and this temperature does not appear to be an upper limit. The performance of the control circuit at higher temperatures and under varied conditions could not be further determined because of failure of the transformer originally used as T-2, Figure 2. This transformer has recently been replaced by the one listed in Table I. Results of further tests and details of operation will be reported by J. E. Bennett.

TABLE I
 COMPONENTS OF POWER SUPPLY FOR ELECTRON
 BOMBARDMENT FURNACE

S	Switch
S-1	Main circuit breaker, 50 amp
S-2	High Voltage
S-3	High Voltage
S-4	3P DT Toggle
S-5	Micro Switch, Operated by S-3
S-6	SPST Toggle
S-7	Push Button Type, ON Black, 115V
S-8	Push Button Type, OFF Red, 115V
S-9	SPST Toggle, Operates Second Timer
S-10	DPST Toggle
S-11	DPST Toggle
S-12	DPST Toggle
S-13	8PDT Operates Servo Motor
S-14	Micro Switch, overload reset
S-15	Circuit Breaker on Stabiline Voltage Regulator
T	Transformer
T-1	F520HB, Chicago, Rectifier Filament, 5VAC, 20A
T-2	Plate Transformer, UTC Type CG-309, 3000/2500/2000 WVDC 1000 maDC
T-3	21F26, Thordarson, 7.5V, 51A, CT
T-4	40V, 40A, Frampton
T-5	Pc8401, Stancor, 6.3V, 2A
H	Choke
H-1	UTC-CG15 10hy, 1000ma
H-2	T20C53, Thordarson
C	Condenser
C-1	20mfd 450V, Electrolytic, Sprague TVL
C-2	2mfd 200V, Paper Aerovox Type P92ZN
C-3	2mfd 3000V, Sprague CR-23
RT	Tubes
RT-1	872 A Rectifier Tube
RT-2	0A2 Regulator Tube
RT-3	5651 Regulator Tube
RT-4	5Y3 Rectifier Tube
L	Light
L-1	Green
L-2	Red
L-3	Amber
L-4	Amber
L-5	Amber
(X)	Connection to Crucible
(F)	Connection to Filament

TABLE I (Continued)

R	Resistor
R-1	100K, 200W, wire wound IRC 10-1/2 H(HO)
R-2	As required to double range of Ammeter
R-3	1/2 or 1 ohm, 1%
R-4	3 Meg ohm
R-5	20K, 25W, w/slider, Type DHA IRC IMM223
R-6	20K, 2W, 5%, IRC Type BT
R-7	75K, 1W, 1%, IRC Type DCF
R-8	10 ohm, 50W, IRC (EP)
R-9	50 ohm, 200W, wire wound
R-10	500K, Dual, Pot, Ohmite #CCU5041
R-11	1K Pot, wire wound, Clarostat, Type 58-1000
R-12	100K, Micro Pot (Borg 205)
R-13	1000 ohm, 3 W, Pot.
Relay-1	DPDT, Power relay, P-2200, 25A
Relay-2	Overload relay X-300-ER with current adjustment
M	Meter
M-1	Voltmeter 0-3000 VDC
M-2	Milliammeter 0-500 ma DC
M-3	Voltmeter 0-150 VAC
M-4	Ammeter 0-50 Amps AC
V-20	V-20 Variac (Filament)
W-20	W-20G2 Variac (High Voltage)
W-2	W-2 Variac, operated by Servo Motor
VR	Stabiline Voltage regulator
SA	Servo Amplifier, Brown 356413-1
MT	Motor, Operated by Servo Amplifier, Brown 76750-3

PART II

TORSION TEST SYSTEM

Introduction

The vapor pressures of metals have been measured in numerous ways; among the most common is the Knudsen method (9). In a Knudsen determination the number of moles of the vapor n effusing in unit time through a unit area is related to the vapor pressure P_k by

$$P_k = (2\pi MRT)^{1/2} \cdot n/W. \quad (1)$$

Where R is the gas constant, T is the absolute temperature, and M is the molecular weight of the effusing species. The Clausing factor W (1) is the probability that a molecule, having entered one end of a hole of finite length, will escape from the opposite end. The Knudsen equation relies on the assumption that the molecular weight of the effusing species is known at any given temperature. Uncertainty of the molecular weight of the effusing species limits the usefulness of the data obtained by this method for thermodynamic calculations.

Several methods for simultaneous determinations of vapor pressures and molecular weights at temperatures obtainable by resistance heating have been developed (11,13,14,19,20). Recently, Searcy and Freeman (18) described a method for simultaneously determining the vapor pressures of metals by the Knudsen and the torsion method in the 1200-2200°K range using radio frequency induction heating. In the torsion method the vapor pressure is related to the torque produced in a suspension

wire by the force resulting from effusing vapors. The torsion method enables one to determine the vapor pressure of a substance without involving the molecular weight in the calculation. The results from the Knudsen method and the torsion method should agree within experimental error if the molecular weight \underline{M} assumed for the Knudsen calculation of \underline{P}_k and the actual effective molecular weight \underline{M}^* of the effusing vapor are the same. Since \underline{P}_k is inversely proportional to the square root of the assumed molecular weight of the effusing vapor, it is related to the actual pressure \underline{P}_t by

$$\underline{M}^* = \underline{M}(\underline{P}_k/\underline{P}_t)^2. \quad (2)$$

If more than one species is effusing, \underline{M}^* is an average molecular weight which is related to the molecular weights of the effusing species by the equation $\underline{M}^* = (a_1 \underline{M}_1^{1/2} + a_2 \underline{M}_2^{1/2} + a_3 \underline{M}_3^{1/2} + \dots + a_n \underline{M}_n^{1/2})^2$ in which a_1 represents the number of molecules having the molecular weight \underline{M}_1 , etc.

In the suspension system described by Searcy and Freeman (18) the effusion cell was suspended from a tungsten wire and was heated by radio-frequency induction. Difficulty was experienced in adapting induction heating to this method; the empty effusion cell was rotated by the electromagnetic field induced by the radio-frequency current. This system could not be heated by electron bombardment because the suspension wire would be required to carry the total emission current and is much too small. Therefore, for electron bombardment heating the suspension system must be independent of the effusion cell.

A suspension system was designed which would allow electron bombardment heating to be employed, and which would enable one to measure small forces such as exerted by effusing vapors. The suspension system

design was based on the principle of the electrodymanometer (4,5,6,17).

A test unit was built that would operate on the same mechanical principle, but which would not be as sensitive or as expensive as the electrodymanometer, and which would answer several basic questions:

1. Will a moving coil operate properly under vacuum for these measurements?
2. Can pressures of 10^{-3} to 10^{-6} atmospheres be measured by use of a suspension system?
3. Will the suspension return to a given zero, or null point, after each measurement, i.e. is the system stable?
4. Can a simple shutter system be designed which would enable the operator to check the zero, or null, point in the middle of a measurement?

Apparatus

A Leeds and Northrup Type 2500 galvanometer was modified by replacing the mirror with a 0.030-inch aluminium tube to which were attached a collector plate on one end and a balancing weight on the other, as shown in Figure 3, and by replacing the 0.0035-inch suspension wire with a 0.0015-inch gold wire. The modified galvanometer was placed in a vacuum system as shown in Figure 4.

Chamber B is a ballast tank to insure constant pressure for the effusion cell, E. The pressure in chamber B can be adjusted to any desired value in the range 1-150 microns by manipulation of valves V₁ and V₂. Evacuation of chamber A to a pressure less than the pressure in B results in a steady stream of air molecules effusing through orifice O. The air molecules pass through a hole in a collimator plate, C, located a known distance, L, Figure 5, from the orifice and coaxial

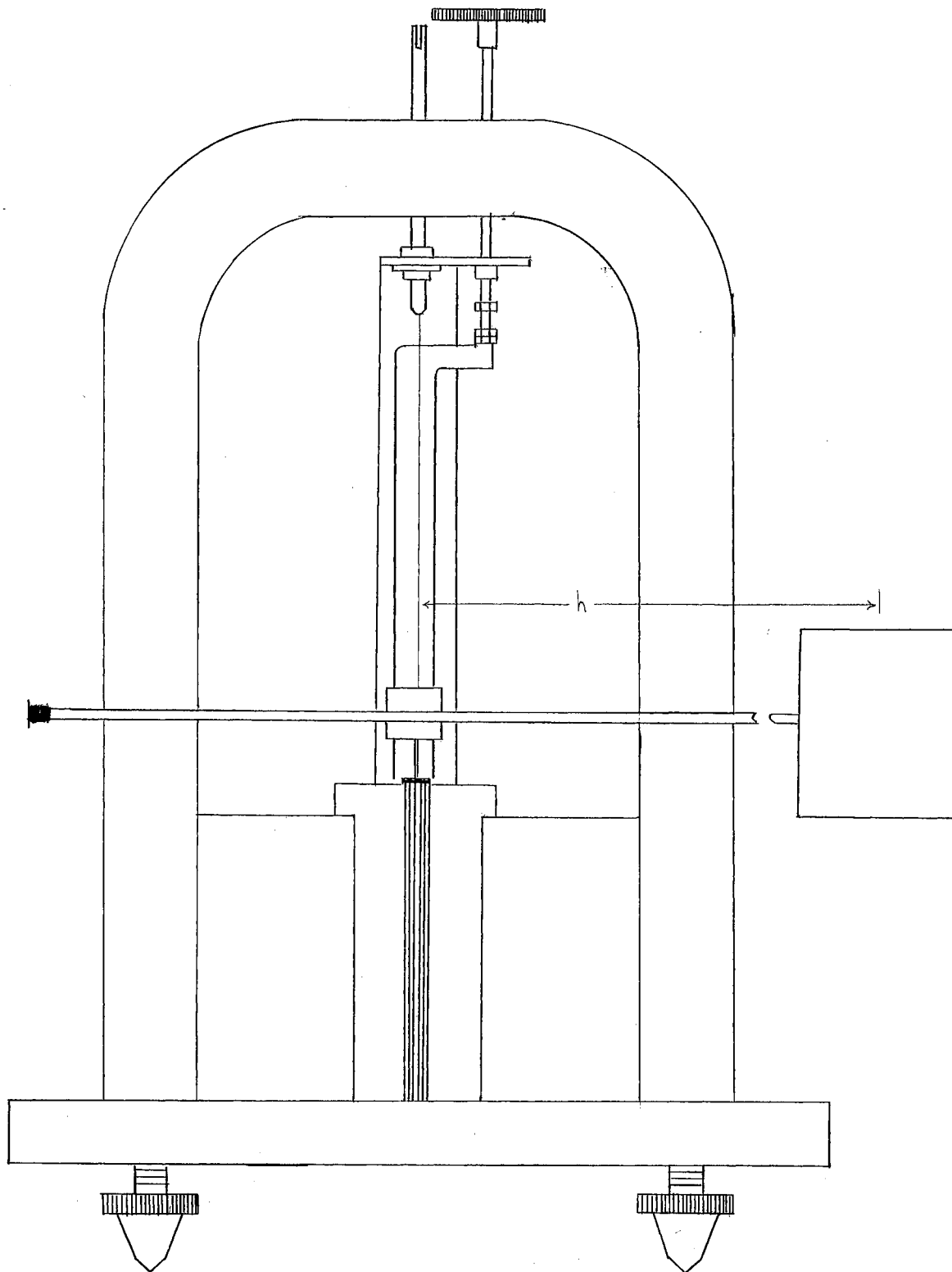


Figure 3. Modified Leeds and Northrup Galvanometer

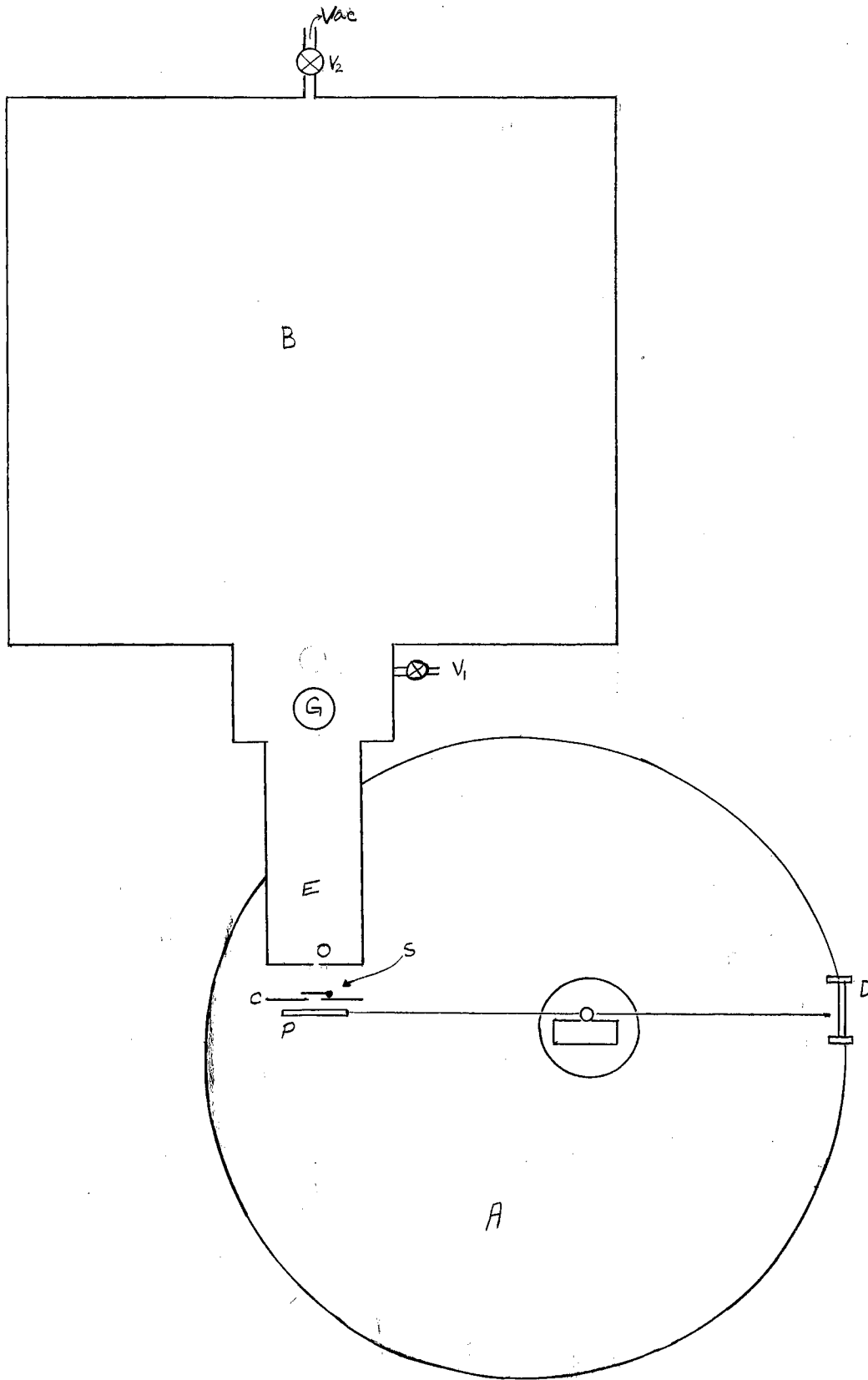


Figure 4. Vacuum Chamber for Torsion Test System

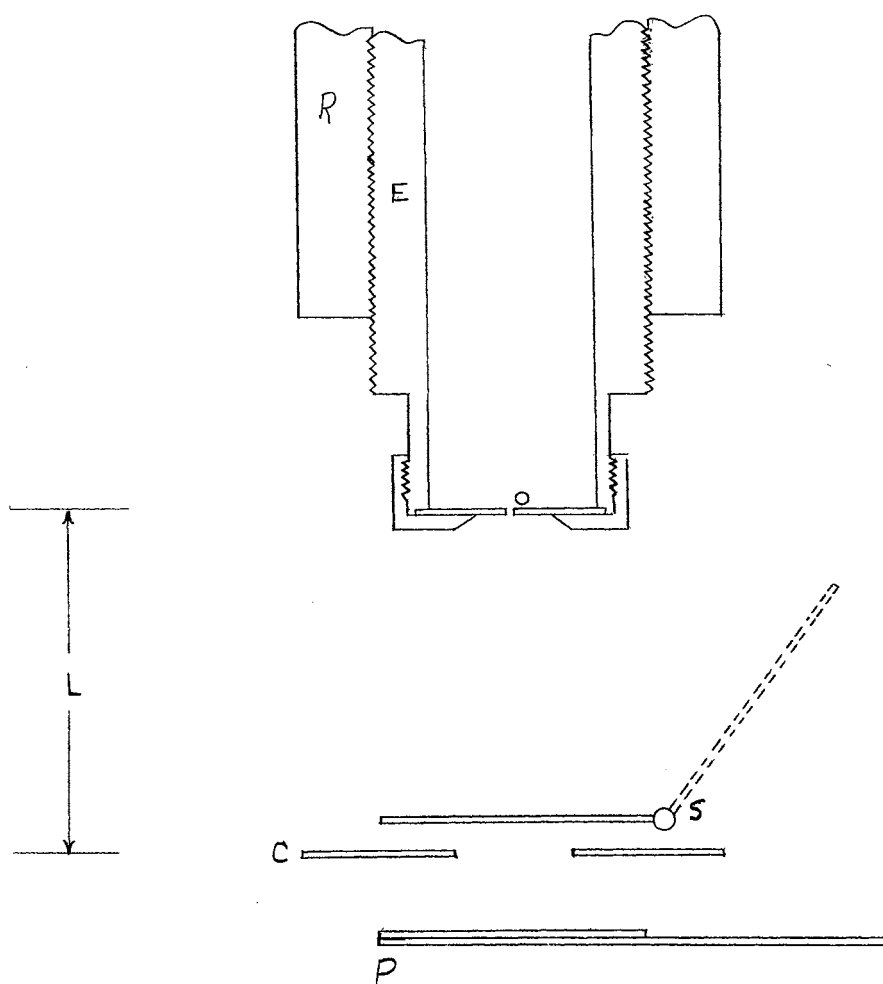


Figure 5. Effusion Cell and Collimator of Torsion Test System

with the orifice. The collector plate, P, completely covers the hole in the collimator plate, C, as shown in Figure 5. The force exerted by the air molecules upon striking the collector plate, P, tends to move the collector plate away from the zero point. Through the application of current to the modified galvanometer, the collector plate can be returned to the zero point.

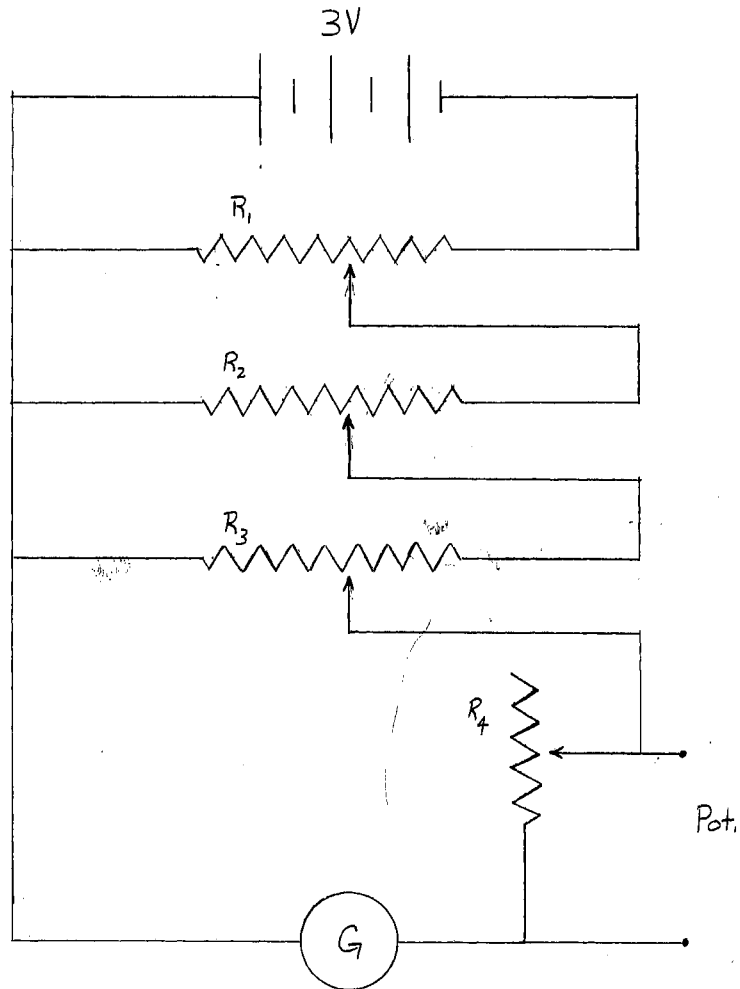
The shutter, S, is shown in Figure 5. When the shutter is in the closed position, represented by solid lines, the air stream is deflected away from the collector plate, and a zero point can be taken. The shutter system enables the operator to make periodic checks on the constancy of the zero point.

An observation port, D, Figure 4, with scale was placed in the side of the vacuum chamber in such a position that the end of the suspension arm was visible directly behind the scale, enabling the operator to establish a zero point.

The effusion tube E, Figure 5, was constructed from brass. The distance L could be adjusted by screwing the effusion tube into the retaining sleeve, R. The orifice plate could be replaced, enabling orifices of different diameters to be employed.

Control Circuit

The current control circuit is shown diagrammatically in Figure 6. Appropriate current was obtained by adjustment of R_1 , R_2 , and R_3 . The resistance represented by R_4 was used to adjust the sensitivity. The voltage drop, across the fraction of R_4 in the circuit, was measured with a potentiometer. The setting of the resistance R_4 was not changed during a given set of determinations.



$R_1 = 1,000$ ohms

$R_2 = 10,000$ ohms

$R_3 = 10,000$ ohms

$R_4 = 50,000$ ohms

G = Modified Leeds and Northrup #2500 Galvanometer

Figure 6. Control Circuit for Torsion Test System

Experimental

The force F_{α} exerted by the molecules which effuse through orifice O and impinge on the collector plate may be calculated from the relations given by Freeman (equation 59, ref. 3):

$$F_{\alpha} = APf_{\alpha}/2 \quad (3)$$

where A is the area of the orifice, P is the pressure in chamber B , and f_{α} is the ratio of the force produced by molecules effusing through a "non-ideal" orifice into the angle α to the total force ($\alpha = \pi/2$) expected under the same conditions except that the orifice is "ideal" (3). The angle α is the semi-apex angle of the right, circular cone which has as its base the opening in the collimator plate and as its height the distance L Figure 5. Equation 3 was derived assuming that the effusing molecules in every case condense on the collector plate. However, in our experimental arrangement, with air as the effusing gas, the molecules do not condense, but rebound; Hence, the force produced is twice that given in Equation 3, or

$$F'_{\alpha} = APf_{\alpha} \quad (4)$$

The torque T produced by this force acting on the collector plate is

$$T = F'_{\alpha} h = APf_{\alpha} h \quad (5)$$

where h is the distance from the center of the collector plate to the suspension wire.

The torque T_g developed in a D'Arsonval galvanometer suspension is given by (2)

$$T_g = BNI\alpha = BN\alpha i/10 \quad (6)$$

where B is the magnetic field strength, N is the number of turns of wire in the suspended coil, α is the area of the coil and I is the current in electromagnetic units and i is the current in amperes.

If the torque \underline{T} exerted by the molecules on the collector plate is exactly counter-balanced by the torque \underline{T}_g developed by current \underline{i} through the galvanometer coil, we may equate (6) and (5), or

$$APf_{\alpha} h = BNi \propto /10$$

and

$$P = \left(\frac{BN \propto}{10 Ahf_{\alpha}} \right) i \quad (7)$$

For a given galvanometer system and a given effusion geometry, the quantities in parentheses in (7) are constants; hence, without knowing their values we may write,

$$P = ki \quad ; \quad k = \left(\frac{BN \propto}{10 Ahf_{\alpha}} \right) = \text{constant} \quad (8)$$

Obviously, then, a plot of \underline{P} , the pressure in chamber \underline{B} , vs. \underline{i} , the current in amps required to maintain the galvanometer on zero, should be a straight line.

In an actual determination the vacuum chamber \underline{A} , Figure 4, was evacuated to a pressure of 2×10^{-5} mm Hg, and the ballast tank \underline{B} was evacuated to 1×10^{-3} mm Hg. The pressure in \underline{B} was then adjusted to any desired pressure by manipulating valves \underline{V}_1 and \underline{V}_2 . There was no appreciable decrease in pressure in the ballast tank, during a period of one hour, due to air effusing through the orifice into the vacuum chamber \underline{A} . Approximately fifteen minutes was required for the determination of each experimental point; hence, the change in pressure during the time required to make a determination could not have significantly influenced the results. The data obtained using a 0.010-inch diameter orifice at a length \underline{L} of 6.0 centimeters is given in Table II. A graph of these data is shown in Figure 7. The experimental points do, indeed, lie along a straight line as predicted by

TABLE II
DATA OBTAINED IN THREE CALIBRATION RUNS

Run No.	Pressure Microns	Current μ amps
1	10	0.496
1	30	1.270
1	79	2.718
1	96	3.254
2	7	0.476
2	29	1.210
2	45	1.647
2	70	2.401
2	79	2.599
2	101	3.194
3	25	0.972
3	50	1.786
3	75	2.698
3	105	3.452

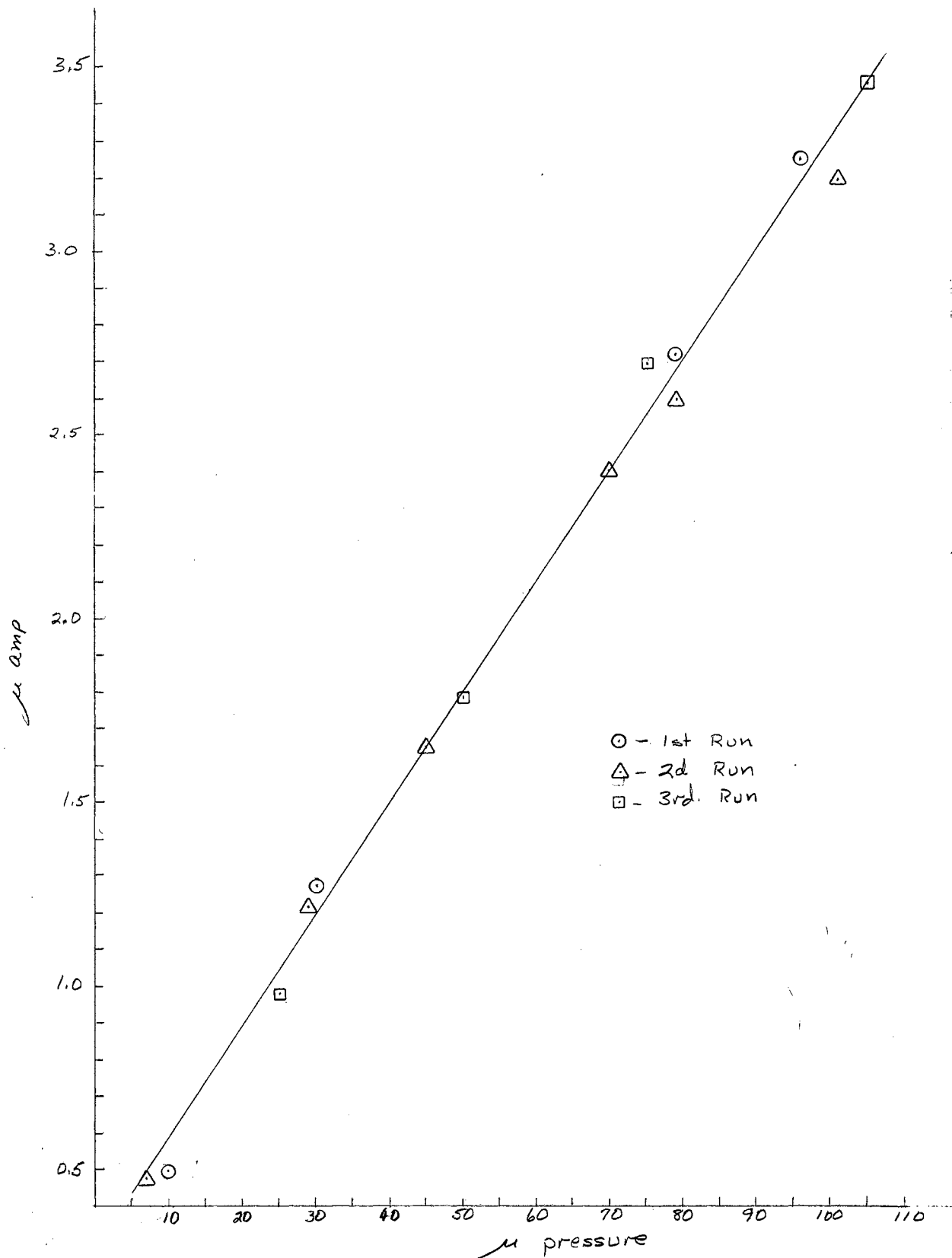


Figure 7. Torsion Test System Calibration Data

Equation 8. The scatter of points along the line is well within satisfactory limits for measurements of such low pressures.

Conclusions drawn from experimentation with the torsion test unit are as follows:

1. A moving coil will function properly in a vacuum.
2. Pressures of 1×10^{-5} atmospheres were measured with the test unit, and a more sensitive suspension would allow even smaller pressures to be determined.
3. The zero point was essentially constant for any given period (maximum deviation over a four-hour period was 0.5%).
4. The shutter device described above was very satisfactory and would enable the operator to determine a zero point at anytime during the duration of a measurement.

PART III

ELECTRODYNAMOMETER

Introduction

The electro-dynamometer consists of a cylindrical coil of wire of a single layer suspended within a larger fixed coil, also cylindrical and of a single layer, the ratio of the radius of each coil to its length being as one to the square root of three. When the two coils have this particular shape and their centers coincide, the expression for the torque, which in general is given by a series of terms, is simplified by the disappearance of all terms after the first and up to the seventh, and this and succeeding terms are usually extremely small if the suspended coil is small in comparison to the stationary coil (15).

If the axes of the two coils are at right angles, the torque is then expressed by the following formula (6):

$$T = \frac{2 \sqrt{7} r^2 N_1 N_2 I_1 I_2}{C} \quad (9)$$

where r is the radius of the suspended coil, and N_1 and N_2 are the whole number of turns of wire on the fixed and suspended coils respectively. I_1 and I_2 are the currents, in electromagnetic units, passing through the fixed and suspended coils respectively, which may or may not be the same. C is one half the diagonal of the fixed coil or $\sqrt{a^2 + b^2}$, a being the radius of the fixed coil and $2b$ its length; as stated above $a/2b = 1/\sqrt{3}$.

The formula may also be written as, $T = HI_1 \times AI_2$, where $H = 2\pi N_1 / C$ and $A = \pi r^2 N_2$. H is the magnetic force at the center of the stationary coil, if unit current flows through it, and A is the sum of the areas of the several turns of the suspended coil.

The equation for the magnetic force at the center of the stationary coil was derived assuming that the current density was the same along the length of the coil, or that the coil was encased in a current sheet. It has been shown by Rosa (17) that the magnetic force calculated from a coil with windings of insulated wire is equivalent to a current sheet to within less than one part per million.

Stationary Coil

The large coil was turned from a four-inch tube of Plexiglas, with a wall thickness of 0.25 inch, which had previously been cured at 100°C for three hours. The form was threaded, 44 threads per inch, to allow the winding to be as even as possible. The windings on the coil consisted of 150 turns of 0.0221-inch diameter, "Nyclad"-insulated, copper magnet wire. The coil diameters were measured with a precision micrometer, which could be read accurately to 0.0001 inch and which was checked with gauge blocks which were accurate to 0.000005 inch. The outside diameter of the wound coil was measured on six different axial planes at each of five equi-spaced positions along the length, giving a total of thirty diameters. These values are given in Table III. One thickness of wire was subtracted from the average outside diameter to give the pitch diameter. The pitch diameter determined by this procedure was 3.9343 inches.

TABLE III
DIAMETERS OF THE STATIONARY COIL

Planes	Positions along the length				
	1	2	3	4	5
I	3.9561	3.9562	3.9565	3.9560	3.9563
II	3.9567	3.9569	3.9570	3.9570	3.9564
III	3.9563	3.9566	3.9570	3.9560	3.9568
IV	3.9560	3.9560	3.9561	3.9568	3.9568
V	3.9560	3.9572	3.9565	3.9564	3.9560
VI	3.9560	3.9555	3.9561	3.9555	3.9560
Average diameter in inches					3.9564
Pitch diameter in inches					3.9343
Pitch diameter in cm					9.9931

The length of the coil from a to b and the distances d, the space covered by 10 turns of wire, Figure 8, were measured with a Gaertner toolmakers' microscope, which measures accurately to 0.0001 inches, and which was checked with gauge blocks which were accurate to 0.000005 inch.

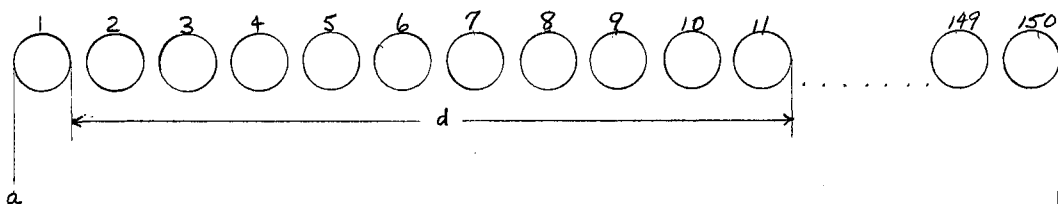


Figure 8. Breadth of "d" Sections on Stationary Coil.

The distances d_2 through d_{15} consisted of 10 turns of wire, which included 10 wires and 10 spaces between the wire. The distance d_1 consisted of 10 turns but had only 9 spaces. The results of 8 measurements

taken along different lines parallel to the axis are recorded in Table IV. The average length of each distance \underline{d} is shown in Table V.

The strength of the magnetic field at the center of the coil when unit current (emu) flows through it is given by

$$H = \frac{4\pi N_1}{\sqrt{D^2 + L^2}} = \frac{2\pi N_1}{C} \quad (10)$$

where \underline{N}_1 is the number of turns, \underline{D} the pitch diameter and \underline{L} the length of the coil. To use this formula, one must assume that the winding is regular. Rosa (17) has shown that the effect of irregular winding on the magnetic force at the center of a coil is appreciable in precise work and a correction must be applied.

A good approximation to a correction for the effect of irregular winding may be made by dividing the winding into a number of sections and calculating the magnetic effect at the center of the entire coil due to each section by

$$H_i = \frac{2\pi n_i}{x_i - x_{i+1}} \left(\frac{x_i}{\sqrt{a^2 + x_i^2}} - \frac{x_{i+1}}{\sqrt{a^2 + x_{i+1}^2}} \right) \quad (11)$$

where \underline{n}_i is the number of turns of wire per section, \underline{x}_i and \underline{x}_{i+1} are the perpendicular distances of the edges of the section from the center of the coil. Then $\underline{x}_i - \underline{x}_{i+1}$ is equal to the breadth of the section. \underline{a} is the mean pitch radius of the winding. The distances \underline{x}_i and the value of \underline{H}_i for each section are given in Table VI.

The strength of the magnetic field, \underline{H} , calculated from Equation 10, not corrected for irregular winding, is 142.586. When \underline{H} is corrected for irregularity in the windings the value obtained is 142.566, as shown in Table VI. Therefore the torque produced is changed by 0.020 I_1 , or the expression for the torque becomes

$$T = (H - 0.020) I_1 A I_2. \quad (12)$$

TABLE IV

BREADTH OF d SECTIONS OF STATIONARY COIL
(MEASUREMENTS GIVEN IN INCHES)

d	Windings	Measurement Number			
		1	2	3	4
1	0- 10	0.2269	0.2266	0.2259	0.2266
2	11- 20	0.2269	0.2267	0.2263	0.2266
3	21- 30	0.2274	0.2278	0.2283	0.2277
4	31- 40	0.2279	0.2274	0.2278	0.2276
5	41- 50	0.2273	0.2262	0.2266	0.2266
6	51- 60	0.2264	0.2267	0.2267	0.2270
7	61- 70	0.2278	0.2289	0.2274	0.2269
8	71- 80	0.2260	0.2300	0.2273	0.2277
9	81- 90	0.2280	0.2223	0.2275	0.2273
10	91-100	0.2277	0.2283	0.2276	0.2271
11	101-110	0.2273	0.2267	0.2272	0.2278
12	111-120	0.2269	0.2272	0.2270	0.2267
13	121-130	0.2275	0.2270	0.2277	0.2278
14	131-140	0.2270	0.2268	0.2264	0.2265
15	141-150	0.2256	0.2276	0.2274	0.2272
	Total	3.4066	3.4062	3.4071	3.4071

d	Windings	Measurement Number			
		5	6	6	8
1	0- 10	0.2265	0.2265	0.2270	0.2259
2	11- 20	0.2268	0.2267	0.2272	0.2278
3	21- 30	0.2275	0.2271	0.2271	0.2266
4	31- 40	0.2278	0.2272	0.2274	0.2273
5	41- 50	0.2273	0.2281	0.2270	0.2275
6	51- 60	0.2266	0.2275	0.2274	0.2275
7	61- 70	0.2278	0.2263	0.2270	0.2265
8	71- 80	0.2266	0.2269	0.2273	0.2276
9	81- 90	0.2279	0.2282	0.2275	0.2278
10	91-100	0.2267	0.2271	0.2271	0.2268
11	101-110	0.2270	0.2271	0.2268	0.2270
12	111-120	0.2269	0.2275	0.2286	0.2280
13	121-130	0.2277	0.2276	0.2262	0.2270
14	131-140	0.2268	0.2266	0.2272	0.2268
15	141-150	0.2273	0.2271	0.2266	0.2278
	Total	3.4072	3.4075	3.4074	3.4079

TABLE V
AVERAGE BREADTH OF d SECTIONS OF
STATIONARY COIL

d	Average Length, inches	Average Length, cm.
1	0.2265	0.5753
2	0.2269	0.5763
3	0.2274	0.5776
4	0.2276	0.5781
5	0.2271	0.5768
6	0.2270	0.5766
7	0.2273	0.5773
8	0.2272	0.5771
9	0.2274	0.5776
10	0.2272	0.5771
11	0.2271	0.5768
12	0.2274	0.5776
13	0.2273	0.5773
14	0.2268	0.5761
15	0.2271	0.5768
Total	3.4073	8.6545

TABLE VI

THE BREADTH AND LOCATION OF EACH SECTION OF WINDING AND ITS
MAGNETIC FORCE AT THE CENTER OF THE STATIONARY COIL

Section Number d	Number of Turns	Breadth of Section, cm.	Distance from End, cm.	Distance from Center, x_i , cm.	H_i $\times 10^{-2}$
			0.0	-4.3273	0.0
1	10	0.5753	0.5753	-3.7520	0.05919
2	10	0.5763	1.1576	-3.1756	0.06985
3	10	0.5776	1.7292	-2.5980	0.08165
4	10	0.5781	2.3073	-2.0199	0.09406
5	10	0.5768	2.8842	-1.4431	0.10600
6	10	0.5766	3.4608	-0.8665	0.11618
7	10	0.5773	4.0381	-0.2892	0.12308
8	10	0.5771	4.6152	0.2879	0.12554
9	10	0.5776	5.1928	0.8655	0.12309
10	10	0.5771	5.7699	1.4426	0.11618
11	10	0.5768	6.3467	2.0194	0.10602
12	10	0.5776	6.9243	2.5970	0.09407
13	10	0.5773	7.5016	3.1744	0.08168
14	10	0.5761	8.0777	3.7504	0.06988
15	10	0.5768	8.6545	4.3273	0.05920
Total	150	8.6545			1.42566

As previously stated, the axes of the movable coil and the stationary coil must be at right angles for the simplified expression for the torque to be valid. To assure that the axes are at right angles and in the same plane, one must either align the two coils coaxially and then rotate the movable coil exactly 90° , or align the axes of the movable coil and the stationary coil in the same plane but perpendicular to one another. This implies that the vertical position of the movable coil must be adjustable. The adjustment mechanism will be considered later in this thesis. It is sufficient to say here that the movable coil was suspended by a 0.00075-inch tungsten wire, which passed through a 0.125-inch opening in the top of the stationary coil. The opening was centered in the exact middle of the winding with the aid of a

centering microscope, and its axis was coincident with a diameter of the coil.

The first method of aligning was accomplished by placing in the ends of the stationary and movable coils plugs with a 0.010-inch hole in the exact center of each. Then, if the axes of the two coils are in the same plane and coincident, one may sight with a telescope along the common axis. The movable coil can then be rotated 90° by employing a cubical mirror which will be discussed later. The second method was accomplished by drilling in the stationary coil two 0.062-inch holes, one at each end of a diameter which passes through the center of the stationary coil and which is perpendicular to the axis of the opening for the suspension wire.

The 0.062-inch openings were plugged with Plexiglas tubes, which had an internal diameter of 0.010 inch. With the aid of a telescope one could, after aligning the movable coil, sight through the holes along the diameter of the stationary coil. To align the coils by either method described, the centers of the two coils must be coincident and the axes must be in the same plane.

The two methods for aligning the two coils were devised and built into the apparatus because one could not foresee which method of alignment would be the more convenient. Regardless of which method was used the final position of the little coil would be the same.

The placing of openings in the stationary coil necessitated the displacement of the wires around the openings. The effect of this displacement of wires on the magnetic field at the center had to be determined in order to apply the appropriate correction.

First let us consider the effect of the 0.125-inch opening for the suspension wire. As shown in Figure 9, six wires had to be displaced for the 0.125-inch opening.



Figure 9. Winding Displacement on the Stationary Coil.

The actual displacement for each wire is given in Table VII.

TABLE VII
WIRE DISPLACEMENT FOR OPENINGS IN STATIONARY COIL

Opening	Number of Wires Displaced	Displacement Inches	Direction of Displacement
0.125	1	0.062	Horizontal, left
0.125	1	0.062	Horizontal, right
0.125	1	0.040	Horizontal, left
0.125	1	0.040	Horizontal, right
0.125	1	0.018	Horizontal, left
0.125	1	0.018	Horizontal, right
0.125	2	0.0681	Radial
0.125	2	0.0454	Radial
0.125	2	0.0227	Radial
0.062	4	0.0454	Radial
0.062	4	0.0227	Radial

By the horizontal displacement of the same number of wires the same distance in opposite directions, the effect upon the magnetic field is counterbalanced and no correction need be applied (17).

It has been shown by Rosa (17), that dH/H for radial displacement of one complete turn of wire is equal to $da/7a$, where H is the strength of the magnetic field and a is the radius of the coil. However, the displacement in our case is for 0.512 inch along the periphery, as measured with the Gaertner toolmakers' microscope, or $0.512/12.4294$ of one complete turn. Also these six wires exert only 5.267% of the total force at the center; hence, the relative change in the total force due to the radial displacement of the wires is

$$\frac{dH}{H} = \frac{2}{7} \cdot \frac{0.512}{12.4294} \left(\frac{(0.0681 + 0.0454 + 0.0227)}{1.9671} \right) (0.05267)$$

or $\frac{dH}{H} = 0.00004$ (13)

The effect due to the horizontal displacement of the eight wires for the two 0.062-inch openings is zero. Each of the eight wires was displaced 0.362 inch along the periphery as measured with a Gaertner toolmakers' microscope, and the eight wires exert 7.020% of the total force at the center. Therefore, the effect on the magnetic field created by the displacement of the eight wires for the two openings is

$$\frac{dH}{H} = \frac{4}{7} \cdot \frac{0.362}{12.4294} \left(\frac{(0.0454 + 0.0227)}{1.9671} \right) (0.0702)$$

or $\frac{dH}{H} = 0.00004$ (14)

The total effect of the three openings on the magnetic force at the center is eight parts in one hundred thousand.

Movable Coil

The movable coil was machined from a one-inch Plexiglas rod, which had been cured at 100°C for three hours. The small coil was also threaded, 44 threads per inch. The windings consisted of 30 turns of 0.0221-inch diameter, "Nyclad"-insulated, copper magnet wire. The

pitch diameter and the length of the small coil were determined in the same manner as they were for the stationary coil and were found to be 0.7860 and 0.6806 inches respectively. The measured diameters are given in Table VIII and the lengths of the winding in Table IX.

TABLE VIII
DIAMETERS OF THE MOVABLE COIL

	1	2	3
0	0.8080 inch	0.8080	0.8080
I	0.8082	0.8082	0.8081
II	0.8082	0.8080	0.8081
III	0.8082	0.8079	0.8080
IV	0.8081	0.8081	0.8082
V	0.8082	0.8082	0.8082
Average Diameter in inches		0.8081	
Pitch Diameter in inches		0.7860	
Pitch Diameter in cm.		1.9964	

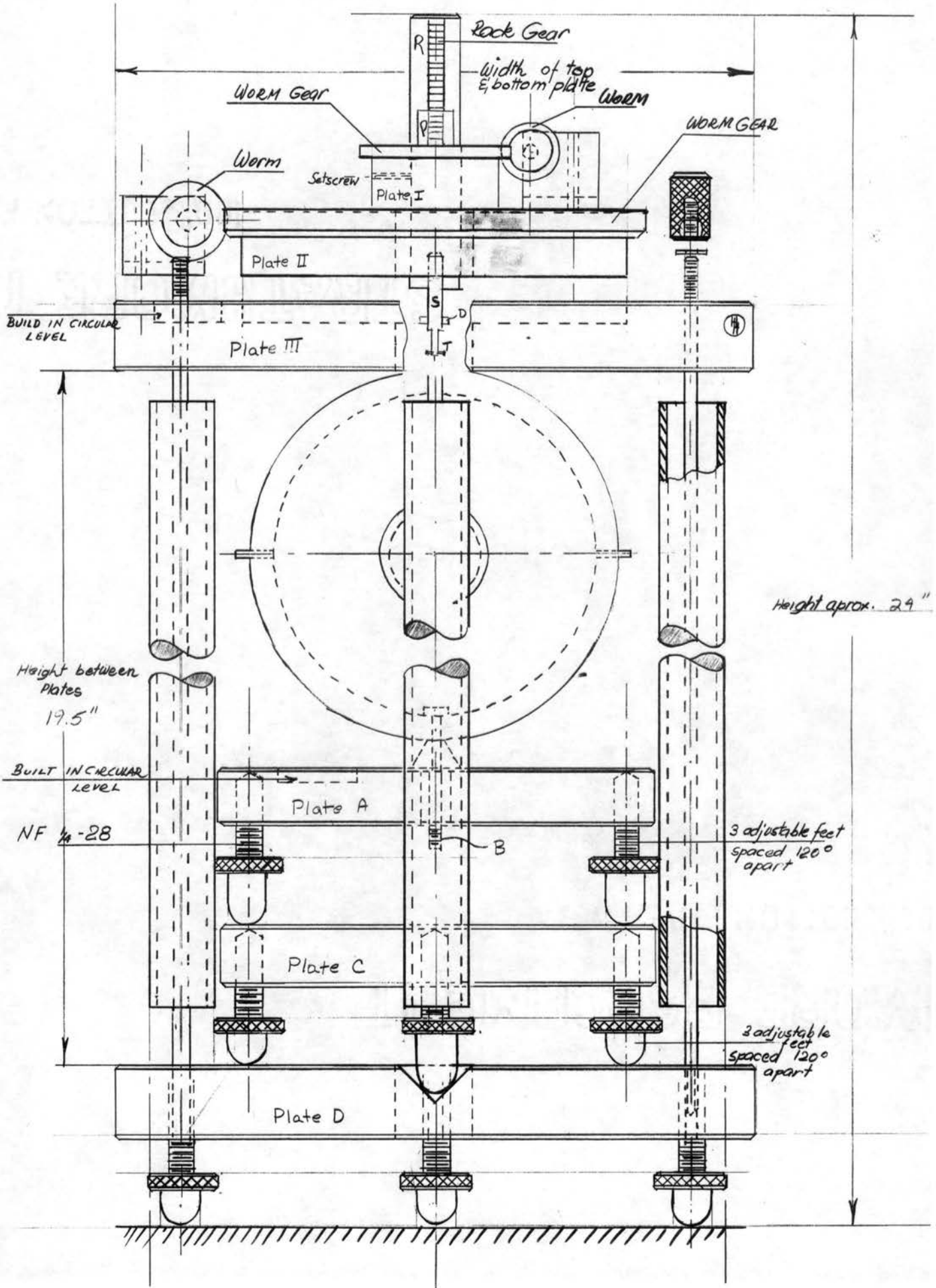
TABLE IX
LENGTH OF WINDING OF MOVABLE COIL

1.	0.6805 inch	5.	0.6809 inch
2.	0.6804	6.	0.6802
3.	0.6803	7.	0.6805
4.	0.6811	8.	0.6806
Average Length in inches		0.6806	
Average Length in cm.		1.7287	

Suspension Adjustments

To enable the operator to align the movable coil in a minimum of time, a number of adjustment have been built into the suspension system, Figure 10. The rack, R, and pinion, P, enable the operator to raise and lower the movable coil a maximum of one inch. The extension arm

Figure 10. Suspension Adjustments



S is a 0.25-inch diameter brass rod, held in place by a set screw. The end of the brass rod has been machined to 0.124 inch so that the cubical mirror could be attached. The cubical mirror is held in place by a small retaining nut. The suspension wire is inserted in a 0.030-inch hole in the tip T and is held in place by two small set screws. Suspension wires of different length may be used by replacing the brass rods with another rod of appropriate length. Since one electrical lead to the movable coil is the suspension wire, the brass rod, S, has been insulated from the rack, R, by incasing the rod in a thin Plexiglas sleeve. The actual electrical connection is made at D, which consists of a small brass ring held in place by a set screw.

Plate I enables the operator to remove the twist in the wire without rotating the movable coil. Rotation of Plate II will rotate the entire suspension system. It appears that there is no need for both of these adjustments on this particular system. However, when the suspension system is to be employed in the vapor pressure measurements, a collector plate and arm will be attached to the movable coil, similar to the one described for the torsion test system. The length of the arm and the geometry of the brass supports forbid rotation of the movable coil more than 110 degrees; therefore, these two adjustments, one to relieve the twist in the suspension wire and one to rotate the movable coil into its correct position for alignment, will be necessary.

The stationary coil was supported by three brass plates as shown in Figure 10. The coil was held fast to Plate A by retaining bolts B. Plate A was supported by three adjustable feet, which were set in "V" grooves on Plate C. This enables one to remove the coil and Plate A

and return them to exactly the same location on Plate C. Plate C was supported on Plate D by three adjustable feet, only one of which was placed in a "V" groove on Plate D. This allows Plate C to be moved as shown in Figure 11.

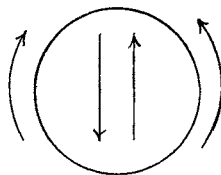


Figure 11. Degrees of Freedom of Stationary Coil

These adjustments were deemed necessary to insure that the suspension wire passed through the center of the opening in the top of the stationary coil.

As shown in Figure 10, leveling bulbs have been placed on Plate A of the stationary coil assembly and on Plate III of the adjustment assembly. These make it possible for the critical parts of the assemblies to be leveled by proper adjustment of the respective feet.

Suspension Wires

The suspension wire employed in these measurements was a 0.00075-inch diameter tungsten wire, 23 centimeters in length, purchased from North American Phillips Co., Inc., Lewiston, Maine.

The small diameter of the wire resulted in difficulty in attaching the wire to the small coil and to the adjustment mechanism. To overcome this difficulty, approximately one-half inch of the wire at each end was copper-plated to a diameter of 0.029 inches. Each plated end was then inserted into a 0.030-inch hole drilled in a 0.060-inch

diameter brass rod and held in place by two small set screws.

To calibrate the wire, a brass cylinder of known moment of inertia was suspended by the wire and the period of oscillation determined.

The moment of inertia, I , of a body made up of several concentric cylindrical sections is given by (7):

$$I = (m_1 r_1^2 + m_2 r_2^2 + \dots + m_i r_i^2) / 2 \quad (15)$$

where m_i is the weight and r_i is the radius of the i th section. The cylinder used in these measurements is shown in Figure 12 and the dimensions are given in Table X. The calculated moment of inertia was 4.9671g cm^2 .

The brass cylinder was suspended by the wire, which was fastened to T , Figure 10, and the period was determined by the well-known method of coincidences. The time required for ten complete periods was measured with a Standard Electric Time Company clock, Model S-1, which could be read accurately to 0.01 second. Ten periods were measured instead of one to eliminate the error introduced in starting and stopping the clock. A typical set of data is given in Table XI.

TABLE X
DIMENSIONS OF BRASS CYLINDERS

Radius	Length	Weight
$r_1 = 0.2395 \text{ cm.}$	$l_1 = 0.6960 \text{ cm.}$	$m_1 = 1.0556 \text{ gm}$
$r_2 = 0.9119$	$l_2 = 0.5398$	$m_2 = 11.8720$
$r_3 = 0.0656$	$l_3 = 0.7112$	$m_3 = 0.188$

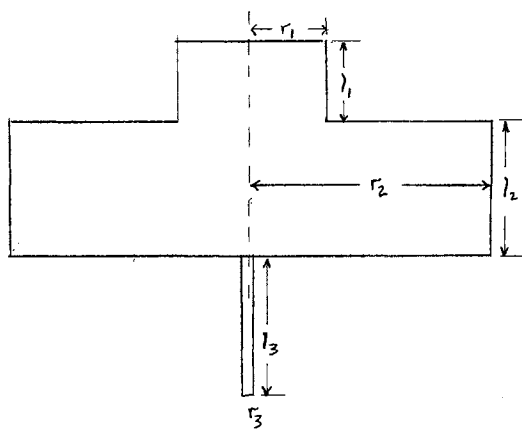


Figure 12. Brass Cylinder
for Calibration
of Cubical
Mirror

TABLE XI
PERIOD OF OSCILLATION FOR SUSPENSION WIRE

Number of Periods	Time, seconds
10	477.02
10	478.82
10	480.91
10	477.77
10	477.53
10	479.12
10	480.45
10	478.23
10	480.70
10	482.39
Average	479.29
Average period = $t =$	47.929

The torsion constant, \underline{T}_k , of the wire can be calculated from the following formula,

$$\underline{T}_k = 4\pi^2 \underline{I} / \underline{t}^2 \quad (16)$$

where \underline{I} is the moment of inertia of the cylinder and \underline{t} is the period of

one oscillation. The torsion constant for the wire used in these measurements was found to be 0.08533 dyne-cm/radian.

Cubical Mirror

To insure the rotation of very nearly 90 degrees and the accurate determination of this angle the following scheme was employed: A small glass cube with aluminized sides and a 0.124-inch hole in the center, parallel to the aluminized sides, was placed on a rotary table of a Bridgeport milling machine. The rotary table was equipped with a 0.25-inch spindle in its center. The upper end of the spindle had been machined to 0.123-inch diameter and threaded. This allowed the cubical mirror to be held firmly in place and also placed the axis of the cube exactly in the center of the rotary table. The rotary table could be rotated 360° and could be read accurately to 0.1%. However, the rotary table was used only in estimating the 90° angle and not for absolute measurements.

Opposite two sides of the cubical mirrors at a distance of 94.0 centimeters from the center of rotation, two telescopes and scales were set up at the same level as the mirrors, Figure 13. As a reference point, the scale mark 1.00 of Telescope I was chosen. The cubical mirror was then rotated, setting the face toward Telescope I always on the 1.00 scale mark and noting the reading of the other face by Telescope II. The sides of the cube were marked as shown in Figure 12. The data obtained is given in Table XII.

The reading of Telescope II for 90° should be just the grand average in Table XII. The actual values of the angles are given in Table XIII.

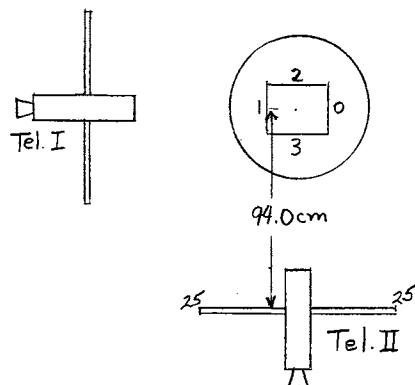


Figure 13. Telescope Arrangement for Calibration of Cubical Mirror.

TABLE XII

CALIBRATION OF GLASS CUBICAL MIRROR

Angle	Telescope I cm.	Telescope II cm.	Average
30	1.00	5.20	
20	1.00	5.28	
21	1.00	5.21	
31	1.00	5.23	5.230
30	1.00	5.20	
20	1.00	5.29	
21	1.00	5.22	
31	1.00	5.24	5.237
30	1.00	5.19	
20	1.00	5.28	
21	1.00	5.20	
31	1.00	5.23	5.225
		Grand Average	= 5.230

TABLE XIII
VALUES OF THE ANGLES ON CUBICAL MIRROR

Angle	Average Reading	Deviation from 90°	Actual Value of Angle	Error, %
30	5.20	+0.009 ^o	90.009 ^o	0.010
20	5.28	-0.015	89.985	0.016
21	5.21	+0.006	90.006	0.007
31	5.23	+0.000	90.000	0.000

Control Circuit

If the two coils were to have the same current flowing through them, they must be wired in series. This meant that the leads to the little coil had to be connected in such a way as to not hinder its rotational movement. To accomplish this a small glass cup, C, Figure 14, filled with a conducting solution, was placed directly below the movable coil, E, with one lead, B, dipping into the cup. The other electrical lead was connected to the suspension wire; thus, the current passed in sequence through the suspension wire, the little coil, the conducting solution A and the lead D. Several liquids, both liquid metals and ionic solutions, were tried as solution A. Both Hg and a low-melting Ga alloy proved to be unsatisfactory because of their high surface tension. Among the ionic solutions tried were saturated solutions of LiCl in ethanol and in methanol, using Cu electrodes, and a saturated KCl solution using Ag-AgCl electrodes. However, these systems proved unsatisfactory because of large fluctuations in the current which resulted when the electrodes became poisoned and/or

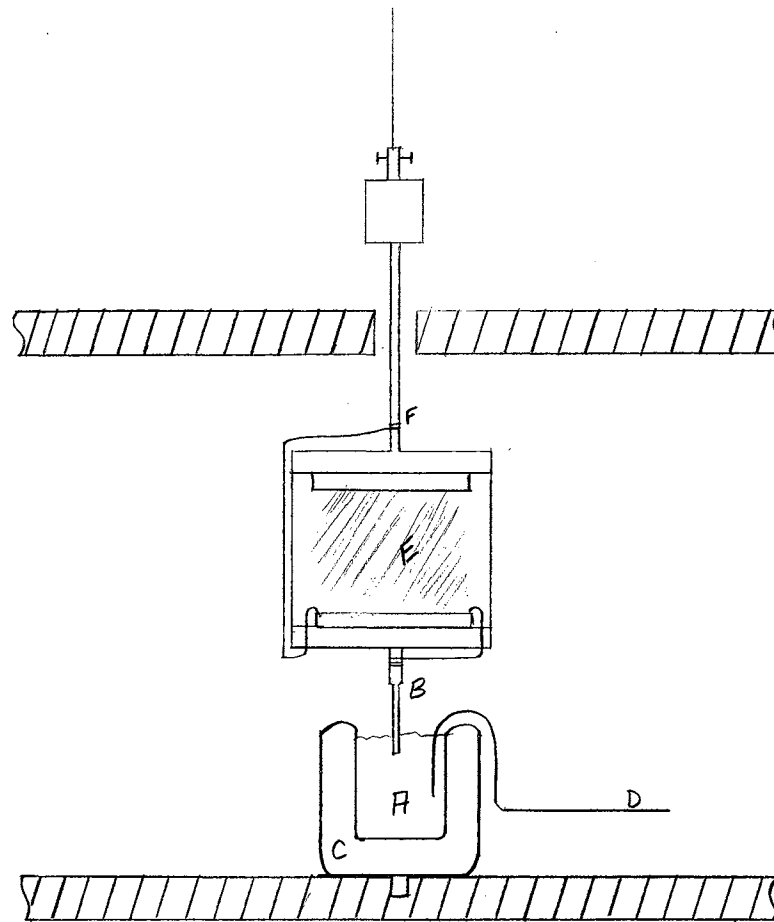


Figure 14. Electrical Connections to Movable Coil

polarized. The only system that allowed rotational freedom for the coil and smooth current flow was a saturated CuSO_4 solution and pure Cu electrodes.

The effect on the torsion constant of the suspension wire produced by current flowing through the wire and with one electrical lead dipping into the CuSO_4 solution was studied and found to be less than 0.1%.

The circuits used in controlling the current flow through the movable coil and the stationary coil are shown in Figure 15, A and B, respectively. A separate control circuit for each coil enabled the operator to vary the current through either coil independently of the other.

Switches S-2 and S-3 are Leeds and Northrup knife switches which allow the direction of current to be reversed in either coil. The resistance R-1 is a standard 10 ohm resistor (General Radio Type 500-B, 0.05%) and the resistance R-2 is a standard 1 ohm resistor (General Radio Type 500-A, 0.15%). The voltage drop across these resistors was measured with a Rubicon potentiometer, Model Number 2730.

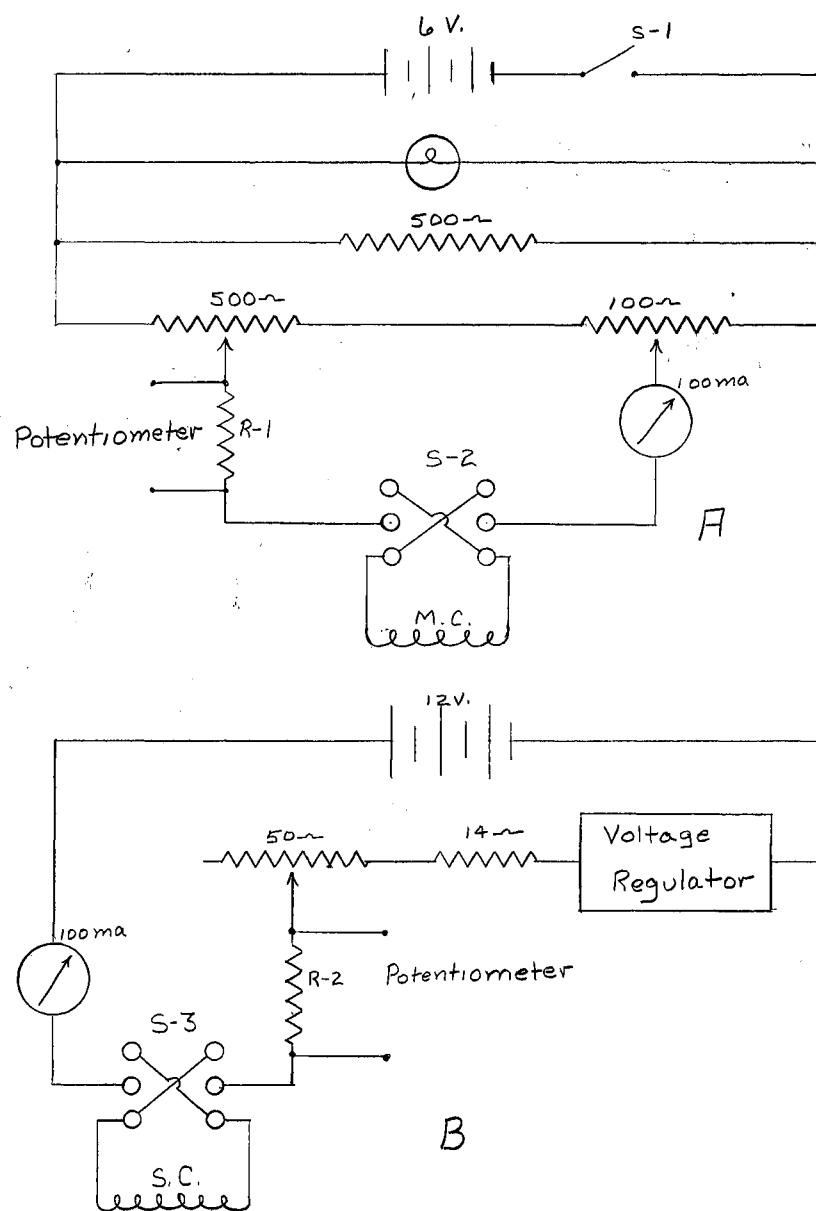


Figure 15. Control Circuit for the Electrodynamometer.

Experimental

To check the combined accuracy of construction of the coils, of calibration of the torsion wire, and of alignment procedures, a comparison of current measured by the electro-dynamometer and by the potentiometer-resistor method was made. The comparison consisted simply of rotating the upper end of the torsion wire through a known angle, passing current through the two coils to generate an exactly opposing torque, measuring the current through the two coils with a potentiometer and a standard resistor, and comparing the measured currents with that calculated from Equation (12).

If numerical values for our two coils are substituted into Equation (12), and the currents expressed in amps, i_1 and i_2 , rather than emu units, I_1 and I_2 , one obtains $T = 133.89 i_1 i_2$. The value of the torsion constant T_k for the wire used in the measurements described below was 0.08533 dyne-cm/radian. The angle γ through which the torsion wire was rotated was, in every case, $90.00 \pm 0.02^\circ$, or $\pi/2 = 1.5708$ radians. If we equate the torque produced by rotating the upper end of the torsion wire, $T_w = T_k \gamma = 0.08533 \pi/2$ and the counteracting torque produced by the electro-dynamometer, $T_e = 133.89 i_1 i_2$, we obtain

$$i_1 i_2 = 0.08533 \pi / (2 \times 133.89) \quad (17)$$

$$\text{or, } (i_1 i_2)^{1/2} = 0.03164$$

$$= 31.64 \text{ milliamps.}$$

Equation (17) is valid if i_1 and i_2 are identically the same current, or if they are completely different.

The current actually measured by potentiometer and resistor in a given measurement is not expected to agree exactly with that given by

Equation (17) because of the influence of the horizontal component of the earth's magnetic field which is of the same order of magnitude as the field produced by the stationary coil with currents of 20-100 milliamps. The effect of the earth's field on the final result, as well as that of perturbations caused by fields around asymmetrically distributed lead wires, may, however, be eliminated, as shown by Guthe (6), by taking the geometrical mean of the currents i_a , i_b , i_c , and i_d which are the values of $(i_1 i_2)^{1/2}$ for the four possible combinations of direction of current in the two coils, e.g. $i_a = (i_1 i_2)_a^{1/2}$, the symbol \underline{a} representing a particular direction of current in the two coils. The resulting geometrical mean current \underline{i}_g should agree with the value in Equation (17).

In an actual determination the two coils were aligned with their axes perpendicular, and a zero point noted on a scale reflected in the cubical mirror at the lower end of the torsion wire. The torsion head was then rotated 90° as measured by the cubical mirror at the upper end of the torsion wire. Mechanical stops prevented the movable coil from rotating more than 6-10 degrees. Current in the stationary coil was maintained at approximately 100 ma, while the current through the movable coil was slowly increased until the coil returned to the zero point. The potential across the two standard resistors (Figure 15) was determined, and therefrom the currents, \underline{i}_1 and \underline{i}_2 , in the two coils were calculated. For a complete experiment this procedure was repeated for all four possible combinations of current direction in the two coils, i.e., for all four combinations of positions of switches 2 and 3, Figure 15.

The results of seven complete experiments are shown in Table 14. The next-to-last column gives the geometrical mean current,

TABLE IV
 COMPARISON OF CURRENT MEASURED BY THE ELECTRODYNAMOMETER AND
 BY THE POTENTIOMETER-RESISTOR METHOD

Experiment Number	Current Direction	Current, Milliamperes				Obs. Calcd.
		i_1	i_2	$(i_1 i_2)^{1/2}$	$(i_a i_b i_c i_d)^{1/4}$	
I	a	100.61 ma.	12.977 ma.	36.13		
	b	99.53	11.960	34.50		
	c	100.55	9.002	30.08		
	d	100.10	10.284	32.08	33.11	1.047
II	a	99.80	13.123	36.18		
	b	99.07	12.285	34.88		
	c	100.25	9.110	30.22		
	d	100.24	10.214	32.00	33.23	1.051
III	a	100.41	13.078	36.23		
	b	99.42	12.162	34.77		
	c	100.69	9.184	30.40		
	d	100.32	10.285	32.12	33.38	1.055
IV	a	99.95	12.982	36.02		
	b	100.70	11.961	34.71		
	c	100.33	9.101	30.22		
	d	99.98	10.146	31.85	33.12	1.047
V	a	100.91	12.887	36.07		
	b	99.94	12.022	34.66		
	c	99.86	9.203	30.32		
	d	101.12	9.989	31.78	33.13	1.047

TABLE IV (Continued)

Experiment Number	Current Direction	Current, Milliamperes				Obs. Calcd.
		i_1	i_2	$(i_1 i_2)^{1/2}$	$(i_a i_b i_c i_d)^{1/4}$	
VI	a	101.10	12.848	36.04		
	b	100.22	11.845	34.45		
	c	100.40	9.325	30.59		
	d	100.17	10.251	32.04	33.21	1.050
VII	a	100.12	13.044	36.14		
	b	100.31	11.986	34.67		
	c	100.61	8.921	29.96		
	d	99.93	10.112	31.79	33.05	1.045

$i_g = (i_a i_b i_c i_d)^{1/4}$, for the four determinations which constitute each experiment. It is this geometrical mean current which should, in each case, have the value 31.64 ma (Equation 17). The last column of Table 14 gives the ratio of observed to calculated values, i.e., the ratio $\underline{R} = i_g / 31.64$.

The values of \underline{R} differ from the desired value of unity by an average of 4.9 percent. However, the precision is better than the accuracy by a factor of ten, the average deviation of \underline{R} from the average of the seven experiments being 0.3 percent.

The reason for the deviation of \underline{R} from unity by five percent is not known at present. The precision of construction of the two coils is 0.1 percent or better. The long term stability of the torsion wire is 0.2-0.3 percent as determined from torsion constants obtained when the wire was first inserted in the apparatus and after three weeks continuous, and not necessarily gentle, use. The possibility of short term shift in zero point of the wire has not been eliminated, but it appears highly unreasonable to obtain the precision in Table 14 if the zero point were drifting appreciably. The two most likely sources of the discrepancy are the procedure for aligning the two coils and, most likely, the copper electrode-copper sulfate arrangement for making electrical contact with the movable coil.

In any case the precision of the apparatus is, as it now stands, sufficient for application to the measurement of the forces exerted on a target by molecules effusing from a Knudsen cell. The precision of 0.5 percent obtained with the electrodynamicometer is better by a factor of ten than that usually obtained in vapor pressure measurements in the range 10^{-3} - 10^{-6} atmosphere. It is expected that others will continue

the development of the electro-dynamometer and of its use in the vapor pressure measurements.

SELECTED BIBLIOGRAPHY

1. Clausing, P., Ann. Physik, (5) 12, 961 (1932).
2. Frank, N. H., Introduction to Electricity and Optics, McGraw-Hill Book Co., Inc., New York, 2d Ed., p 220 (1950).
3. Freeman, R. D., Ph.D. Thesis, Purdue University, (1954).
4. Gray, Andrew, Absolute Measurements in Electricity and Magnetism, MacMillan and Co., New York, p 395 (1921).
5. Gray, Andrew, Phy. Rev., 20, 276 (1905).
6. Guthe, K. E., Bull. B. S., 2, 33 (1906).
7. Hausman, E. and Slack, E. P., Physics, D. Van Nostrand Co. Inc., Princeton, N. J., p 161-174 (1947).
8. Heydman, W. F., M.S. Thesis, Oklahoma State University, (1960).
9. Knudsen, M., Ann. Physik, (4) 28, 999 (1909).
10. Liquid Metals Handbook, Jun. 1952 (Rev. of Jan. 1954) NAVEXOS.
11. Mayer, H., Z. Physik, 67, 240 (1931).
12. McGee, D. W., Ph.D. Thesis, Ohio State University, (1956).
13. Neumann, K. and Volker, E., Z. physik. Chem., A, 161, 33 (1932).
14. Niwa, K. and Shibata, Z., J. Fac. Sci. Hok. Imp. Univ., Ser. III, 3, 53 (1940).
15. Patterson, G. W., Phys. Rev., 20, 300 (1905).
16. Rocco, W. A. and Sears, G. W., Rev. Sci. Instr., 27, 1 (1956).
17. Rosa, E. B., Bull. B. S. 2, 71 (1906).
18. Searcy, A. W. and Freeman, R. D., J. Am. Chem. Soc., 76, 5229 (1954).
19. Volmer, M., Z. physik. Chem., Bodenstein Festband, 863 (1931).
20. Wessel, G., Z. Physik, 130, 539 (1951).

VITA

James Phillip Dawson

Candidate for the Degree of

Master of Science

Thesis: AN ELECTRON BOMBARDMENT FURNACE: AN ELECTRODYNAMOMETER
FOR THE MEASUREMENT OF SMALL FORCES

Major Field: Physical Chemistry

Biographical:

Personal Data: Born in Drummond, Oklahoma, October 18, 1932,
the son of C. Fred and Victoria Ennen Dawson.

Education: Attended grade school in Drummond, Edmond, Oklahoma
City and Weatherford, Oklahoma; graduated from Weatherford
High School in 1950; received the Bachelor of Science
degree from Southwestern State College, Weatherford, Oklahoma
with a major in Chemistry in 1955; received a research
assistantship in the Department of Chemistry at Oklahoma
State University, 1957; completed the requirements for the
Master of Science in May, 1960.

Professional Experience: Entered the United States Army in 1950,
served with the 45th Infantry Division in Japan and Korea,
discharged June, 1952; employed as a chemist in the P-V-T
Laboratory, Thermodynamics Branch, U.S. Bureau of Mines,
Bartlesville, Oklahoma, from August 1955 to April, 1957.